Supporting Information

Polymeric membranes through the self-initiation, self-polymerization for high-performance bioethanol pervaporation

Zhihao Si,[a†] Chang Liu,[a†] Tanlong Xue,[b] Shuai Yang,[a] Yuhui Cui,[a] Yaqi Wang,[a] Di Cai,[a] Peiyong Qin[a*]

[a] National Energy R&D Center for Biorefinery, College of Life Science and Technology, Beijing University of Chemical Technology, Beijing 100029, China.

[b] State Key Laboratory of Chemical Resource Engineering, Beijing Laboratory of Biomedical Materials, College of Materials Science and Engineering, Beijing University of Chemical Technology, Beijing 100029, PR China

*Corresponding author. E-mail address: qinpeiyong@tsinghua.org.cn (P. Qin).

[†] These authors contributed equally to this work.

1. Supplementary materials and methods

1.1 Preparation of the MAPDMS prepolymer

The detailed preparation procedure of MAPDMS prepolymer is given in our previous work.[1] 5.5 g PDMS, 0.9 g KH571, 0.08 g DBTDL, and 0.05 g H_2O were added to the flask. The mixture was stirred under 600 rpm for 12 h at room temperature and decompressed at 60 °C for 12 h. MAPDMS prepolymer was sealed in a jar with a screw cap and stored at 2-8 °C for further use.

1.2 Preparation of the 1173-MAPDMS casting solution and membrane

The 1173-MAPDMS casting solution was fabricated for comparison. Briefly, 5 wt% PI-1173, 5g MAPDMS prepolymer, and 6 g dichloromethane were added to the flask and stirred under 600 rpm for 30 min at room temperature. The mixture was degassed to obtain the 1173-MAPDMS casting solution. The casting solution was sealed in a jar with a screw cap, covered with aluminum foil, and stored at 2-8 °C for further use. The wt% 1173-MAPDMS membrane was the same as the preparation of 1173IPS-MAPDMS membranes

1.3 Evaluations of durability and recycled times

A 5 wt% 1173IPS-MAPDMS membrane irradiated under 165 mW cm^{-2} was used. Firstly, the prepared membrane was fixed in the home-made membrane module (**Fig. S21**). When the PV test was conducted, the membrane module was linked to the feed tank, and the feed solution was circulated by a peristaltic pump. The ethanol concentration in water was maintained at 5 wt%, and the feed temperature was set at 60 °C during PV process. The whole experiment time was 100 h to evaluate the membrane durability, while PV was stopped 5 times and the membrane module was removed to evaluate the recycled times.

1.4 Calculation of energy consumption

The energy required to generate permeate vapor from the feed solution depends on the feed concentration and the separation factor of the membrane. Molecules from the feed side to permeate side requires an endothermic phase transition. Since the separation factor β is never infinite, it takes energy not only to vaporize the target component ethanol but also to vaporize water. The energy required (*Qnorm evap*, kJ kg^{-1}) to evaporate permeate in a PV process, normalized per unit of ethanol permeated, is calculated as follows:[2]

$$Q_{norm}^{evap} = \Delta H_{evap,e} + \Delta H_{evap,w} * \frac{1 - x_e}{\beta * x_e} \tag{1}$$

where $\Delta H_{evap,e}$ (kJ kg^{-1}) and $\Delta H_{evap,w}$ (kJ kg^{-1}) are the evaporation enthalpy of ethanol and water, respectively.

As contrast, the energy consumption (Q'_{norm}, kJ kg^{-1}) based on the heat requirement for evaporation for the removal of 1 kg ethanol from ethanol/water mixtures was estimated as follows:[3]

$$Q'_{norm} = \Delta H_{evap,e} + (\frac{1}{y_e} - 1) * \Delta H_{evap,w} \tag{2}$$

1.5 Gas transport measurement

Pure gas (CO_2, H_2, CH_4, and N_2) permeation tests were carried out by custom-constructed constant-volume/variable-pressure equipment at a temperature of 35 °C and 1 bar based on previous work.[4] The permeability performance was evaluated by pure gas steady-state permeation rate (P, Barrer) as follows:

$$P = \frac{273 \times 10^{10}}{760} \frac{VL}{AT\left(\frac{p2 \times 76}{14.7}\right)} \frac{dp}{dt} \tag{3}$$

where V and L are the volume of the downstream chamber (cm^3) and the membrane thickness (cm), respectively. A and T refer to the effective area of the membrane (cm^2) and the experimental temperature (K), respectively. $p2$ (psia) is the pressure of the feed gas in the upstream chamber. The ideal selectivity $\alpha_{A/B}$ is the ratio of the permeability coefficients of the pure components A and B.[5]

$$\alpha_{A/B} = \frac{P_A}{P_B} \tag{4}$$

2. Supplementary data and figures

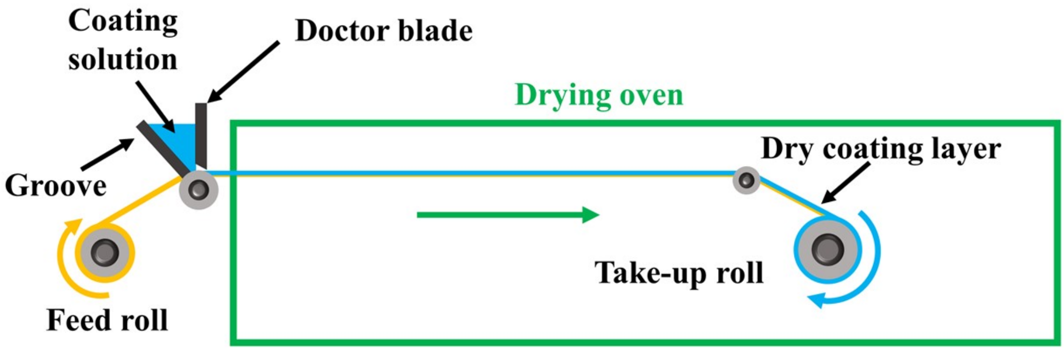

Fig. S1 Schematic of a commercial machine for continuously fabricating membranes.

Table S1. Current reported photo-polymerization systems.

System	Polymerization type	Photoinitiator	Blending method of photoinitiator	Doped amount (wt%)	Wavelength (nm)	Ref.
Acrylate-/epoxide monomers	Cationic/free-radical	PI-819[1]/TAS[2]	Physical	0.4/4	390/450	6
Epoxy resins	Cationic	PI-6992[3]	Physical	4	365	7
Thiol-acrylate	Free-radical	PI-2959[4]	Physical	5	365	8
Di(meth)acrylates	Free-radical	PI-1173	Physical	2	320-390	9
nBA[5]and tBA[6]	Free-radical	AIBN[7]	Physical	-	365	10
PC18A [8]	Free-radical	PI-2959[4]	Physical	0.2	360	11
Acrylate	Free-radical	TPO[9]	Physical	1	365	12
Acrylate	Free-radical	BPA[10]	Physical	1	365	13
DGFA[11]	Cationic	TAS[2]	Physical	2	365	14
PEGDMA[12]	Free-radical	PI-2959[4]	Physical	3	300-500	15

1: Phenyl bis(2,4,6-trimethylbenzoyl)-phosphine oxide
2: Triarylsulfonium hexafluoroantimonate salts
3: Triarylsulfonium hexafluorphosphate salts
4: 2-hydroxy-4′-(2-hydroxyethox)-2-methylpropiophenone
5: *n*-butyl acrylate
6: Tert-butyl acrylate
7: 2-azobisisobutyronitrile
8: Poly(n-octadecyl acrylate)
9: Diphenyl (2,4,6-trimethylbenzoyl)phosphine oxide
10: 4-benzoylphenyl acrylate
11: Diglycidyl furfuryl alcohol
12: Poly(ethylene glycol)dimethacrylate

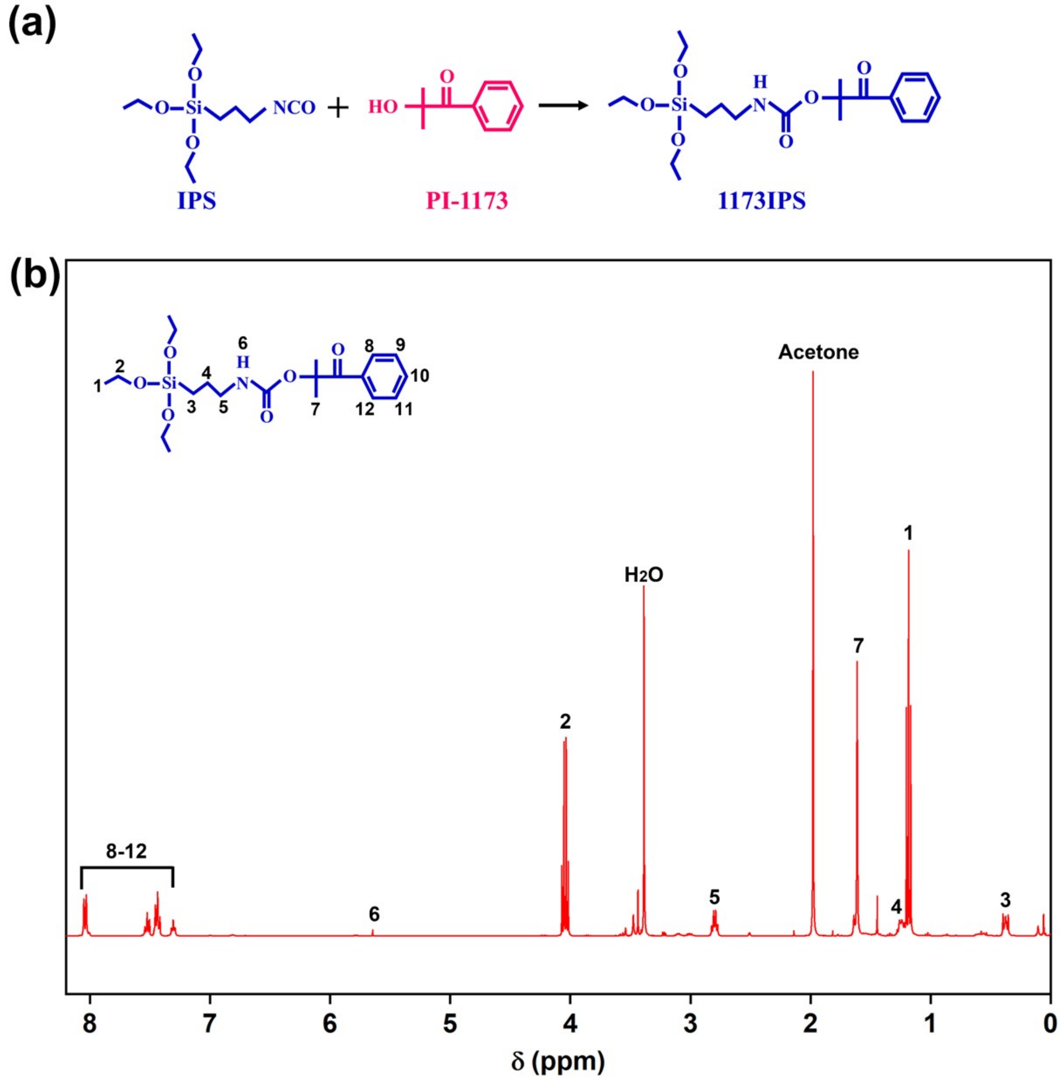

Fig. S2 (a) A schematic diagram showing the synthesis process of 1173IPS. **(b)** ^{1}H NMR spectrum of 1173IPS.

The peak position of ^{1}H NMR (400 MHz, [D_6] DMSO) of 1173IPS: δ 1.18 (t, J = 7.1 Hz, 9H; $SiOCCH_3$), δ 4.03 (q, *J* = 7.1 Hz, 6H; $SiOCH_2$), δ 0.38 (m, 2H; $SiCH_2C$), δ 1.25 (m, 2H; $SiCCH_2$), δ 2.79 (q, *J* = 6.7 Hz, 2H; $SiCCCH_2$), δ 5.65 (s, H; OCONH), δ 1.61 (s, 6H; CCH_3), δ 7.44, 7.52, 8.03 (m, 5H; Ar-H), which are consistent with the anticipated modified 1173 counterpart.[16]

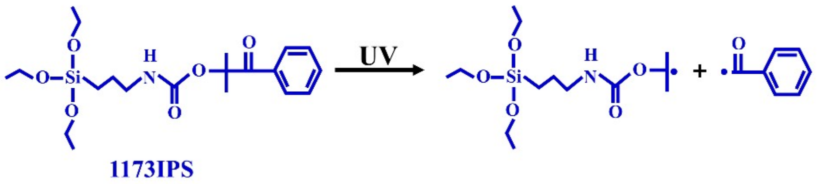

Fig. S3 The initiation process of 1173IPS.

Fig. S4 Casting solutions: **a** physical blending and **b** chemical bonding of PI with PDMS at the same concentration (5 wt%) of PI-1173.

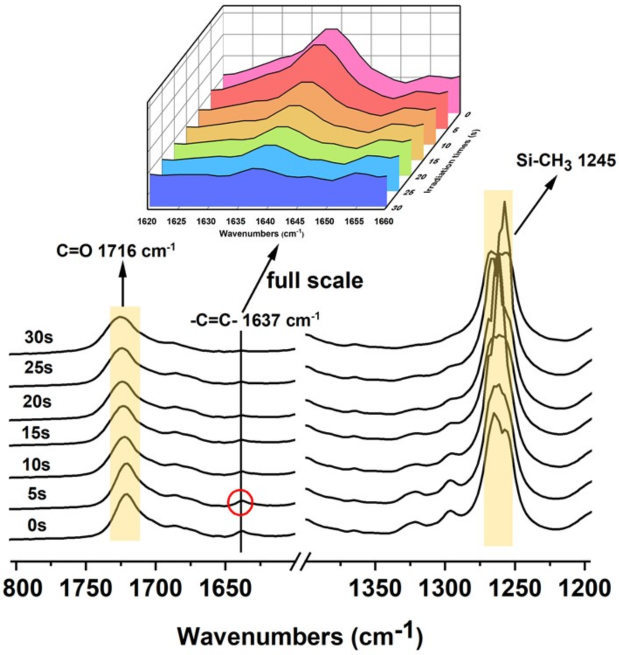

Fig. S5 FTIR spectra of 1173IPS-MAPDMS with 5 wt% PI concentration at 1637cm^{-1} over time.

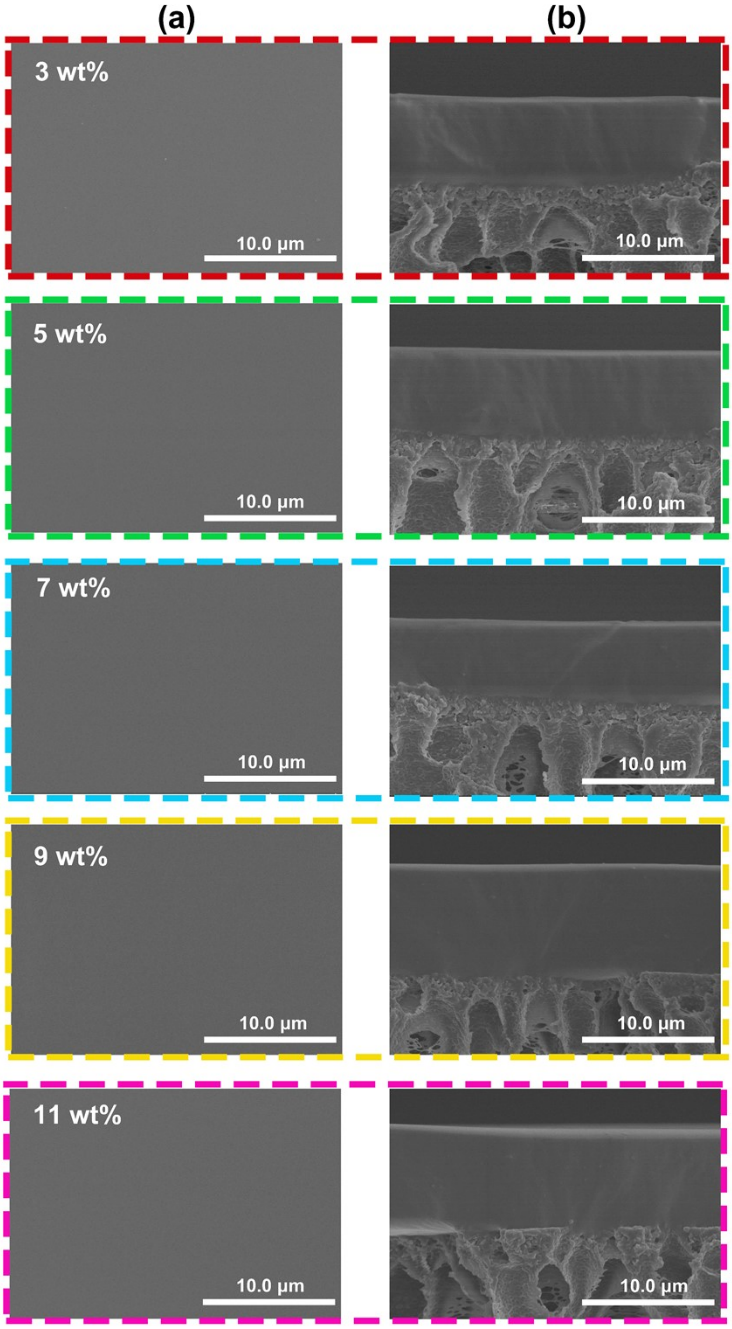

Fig. S6 SEM images of 1173IPS-MAPDMS membranes with 3-11 wt% of 1173IPS concentration under 165 mW cm^{-2} of irradiation intensity (**a** Surfaces and **b** Cross-sections).

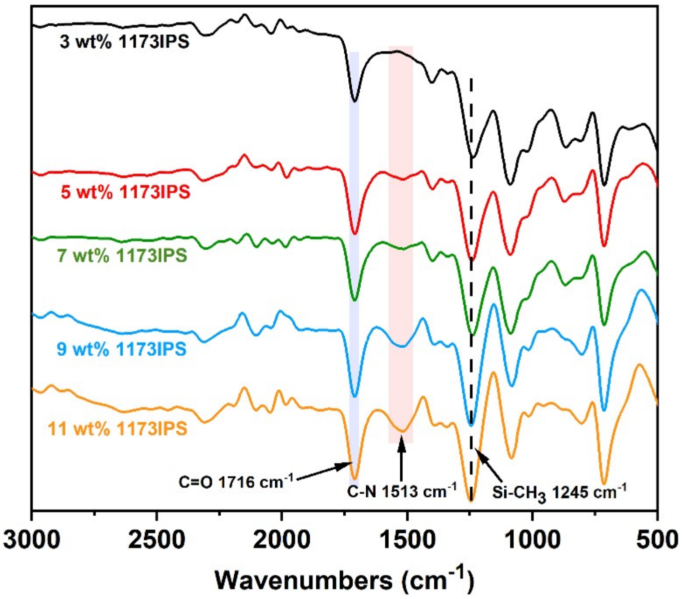

Fig. S7 FTIR spectrum of 1173IPS-MAPDMS membranes with 3-11 wt% of 1173IPS concentration under 165 mW cm^{-2} of irradiation intensity.

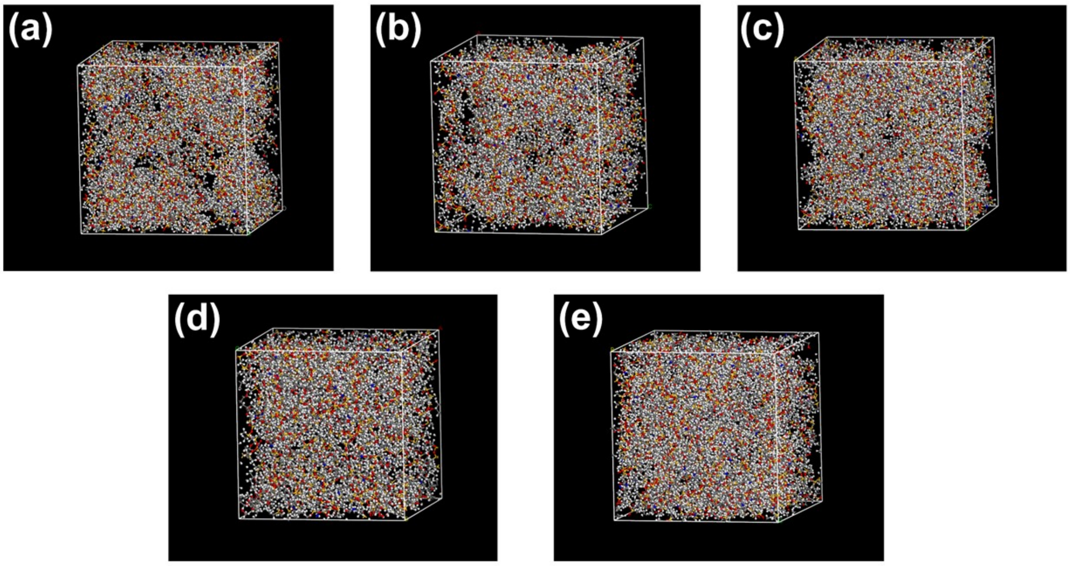

Fig. S8 1173IPS-MAPDMS cells in MD simulation (1173IPS concentration: **(a)** 3 wt%, **(b)** 5 wt%, **(c)** 7 wt%, **(d)** 9 wt%, and **(e)** 11 wt%).

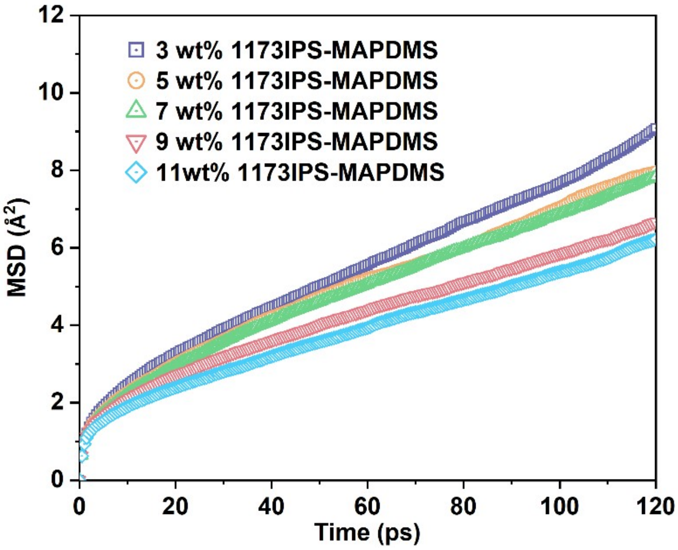

Fig. S9 MSD curves of O atoms in 1173IPS-MAPDMS chains.

Table S2. Free volume properties of membranes with 3-11 wt% of 1173IPS concentration under 165 mW cm^{-2} of irradiation intensity.

1173IPS concentration (wt%)	τ_3 (ns)	I_3 (%)	r_3 (nm)	τ_4 (ns)	I_4 (%)	r_4 (nm)	*FFV* (%)
3	2.16	10.20	0.299	3.720	27.50	0.408	8.95
5	2.09	9.20	0.293	3.697	27.20	0.406	8.62
7	1.92	8.72	0.277	3.551	27.00	0.395	7.73
9	1.90	8.70	0.276	3.510	24.00	0.395	6.97
11	1.81	8.20	0.266	3.475	23.80	0.393	6.71

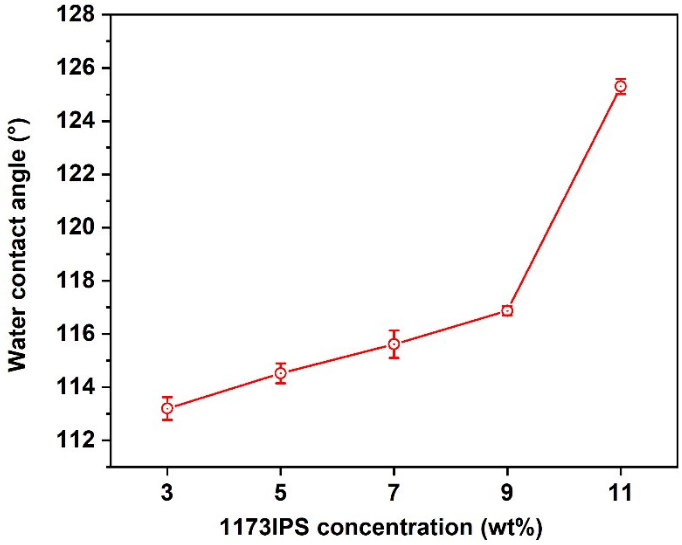

Fig. S10 Water contact angles of membranes with 3-11 wt% of 1173IPS concentration under 165 mW cm^{-2} of irradiation intensity.

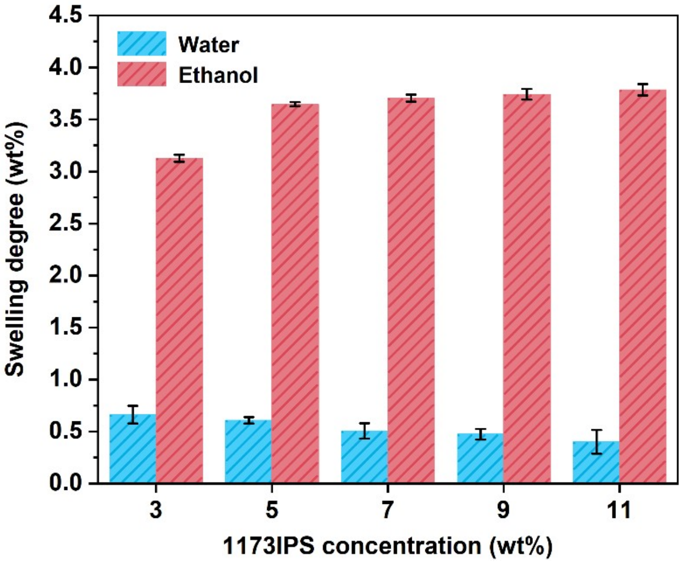

Fig. S11 Swelling degree of membranes with 3-11 wt% of 1173IPS concentration under 165 mW cm^{-2} of irradiation intensity.

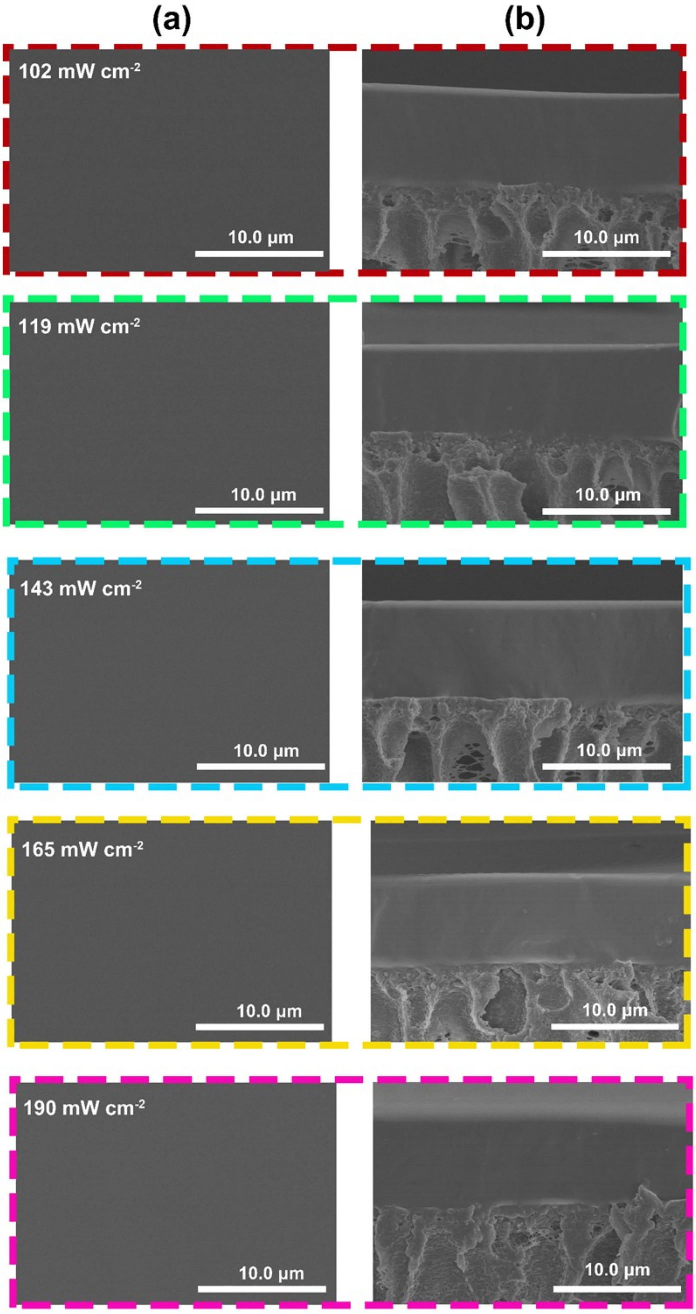

Fig. S12 SEM images of 1173IPS-MAPDMS membranes under 102-190 mW cm^{-2} of irradiation intensity with 5 wt% of 1173IPS concentration (**a** Surfaces and **b** Cross-sections).

Table S3. Free volume properties of membranes under 102-190 mW cm^{-2} of irradiation intensity with 5 wt% of 1173IPS concentration.

Irradiation intensity (mW cm^{-2})	τ_3 (ns)	I_3 (%)	r_3 (nm)	τ_4 (ns)	I_4 (%)	r_4 (nm)	*FFV* (%)
102	1.8	7.77	0.266	3.601	28.33	0.401	8.25
119	1.75	7.47	0.261	3.589	28.29	0.400	8.15
143	1.73	7.10	0.259	3.526	27.40	0.396	7.66
165	1.70	6.61	0.256	3.500	26.31	0.395	7.24
190	1.44	6.55	0.227	3.449	25.95	0.392	6.85

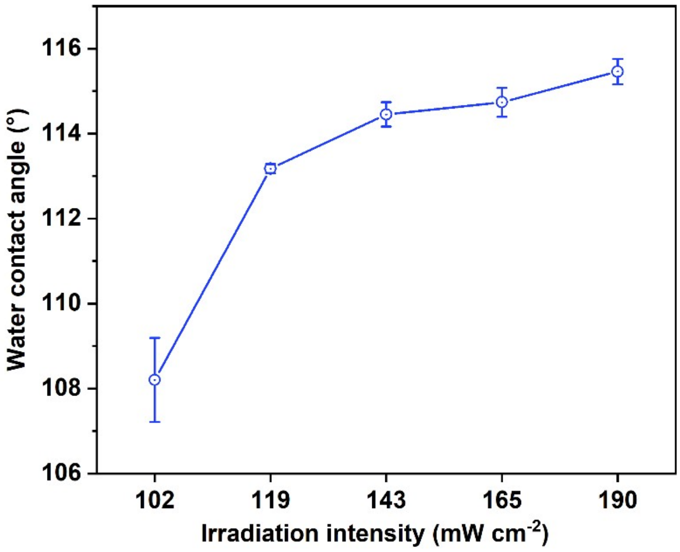

Fig. S13 Water contact angles of 1173IPS-MAPDMS membranes under 102-190 mW cm^{-2} of irradiation intensity with 5 wt% of 1173IPS concentration.

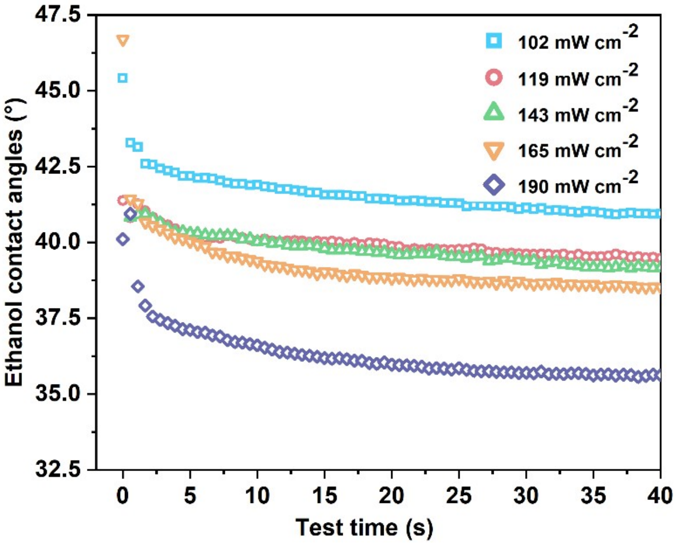

Fig. S14 Dynamical ethanol contact angles of 1173IPS-MAPDMS membranes under 102-190 mW cm^{-2} of irradiation intensity with 5 wt% of 1173IPS concentration.

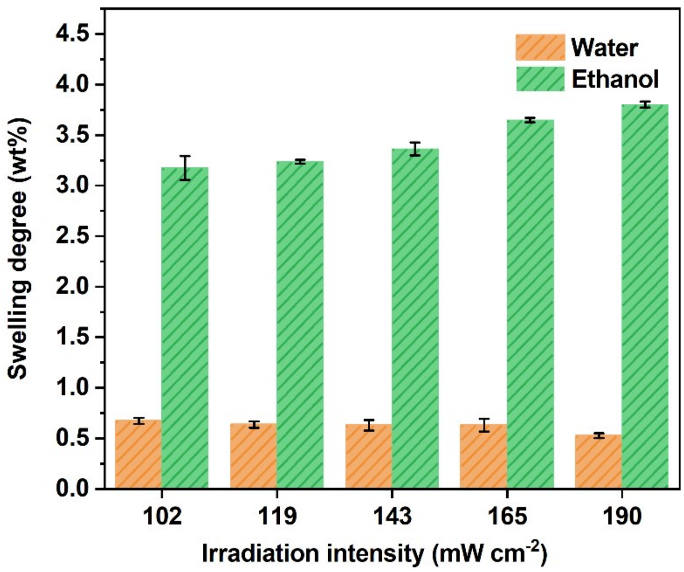

Fig. S15 Swelling degree of 1173IPS-MAPDMS membranes under 102-190 mW cm^{-2} of irradiation intensity with 5 wt% of 1173IPS concentration.

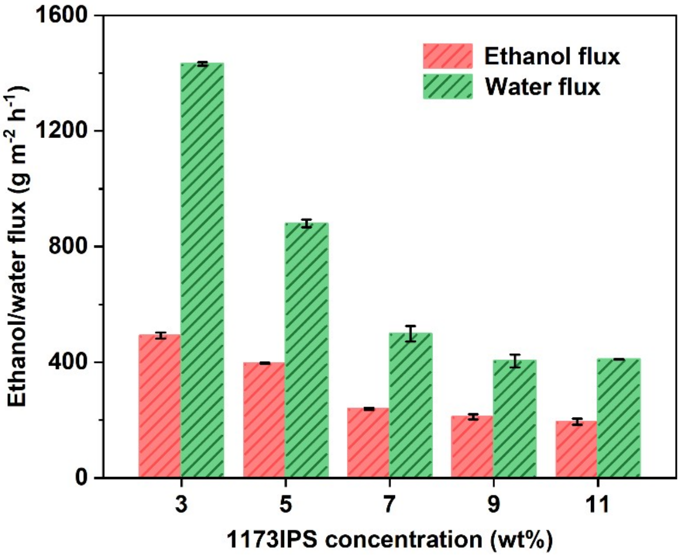

Fig. S16 Effect of 1173IPS concentration (3-11 wt%) on water, ethanol flux under 165 mW cm^{-2} of irradiation intensity.

Table S4. Separation performance of 1 wt% and 13 wt% 1173IPS-MAPDMS membranes.

Membrane	Feed temp. (°C)	Ethanol conc. (wt%)	Total flux (g m^{-2} h^{-1})	Separation factor	*PSI*
1 wt% 1173IPS-MAPDMS	60	5	2222	5.8	10666
13 wt% 1173IPS-MAPDMS	60	5	542	8.6	4119

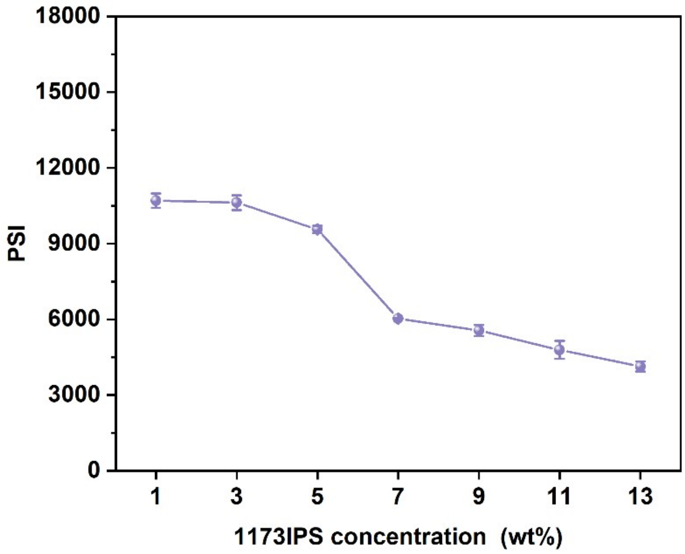

Fig. S17 Effect of 1173IPS concentration on PSI values under 165 mW cm^{-2} of irradiation intensity.

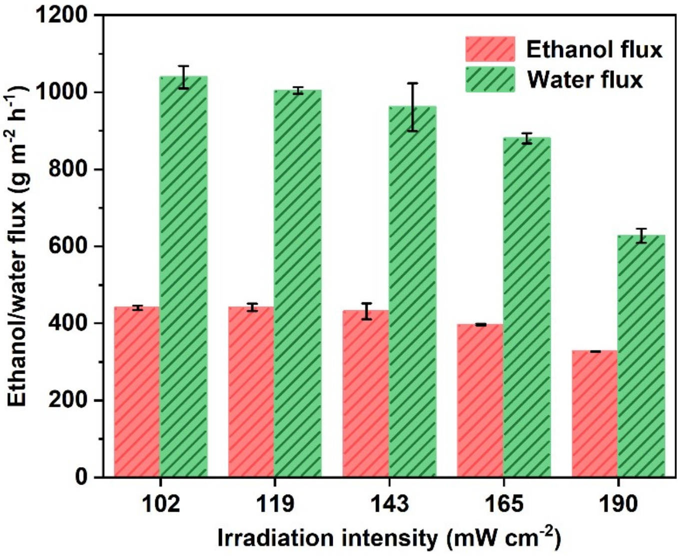

Fig. S18 Effect of UV irradiation intensity (102-190 mW cm^{-2}) on water, ethanol flux with 5 wt% 1173IPS-MAPDMS.

Table S5. The partial vapor pressures of components feeding 5 wt% ethanol/water solution at different temperature (data is acquired from Aspen 11.0 using the NRTL model).

Feed temperature (°C)	Ethanol		Water	
	p_0^1 (Pa)	p_1^2 (Pa)	p_0^1 (Pa)	p_1^2 (Pa)
30	904.89	10.82	4165.45	69.18
40	1595.97	11.53	7243.29	68.47
50	2676.99	11.71	12115.45	68.29
60	4407.70	11.99	19555.87	68.01
70	6890.57	12.24	30586.86	67.76

1: Partial vapor pressure on the feed side.

2: Partial vapor pressure on the permeant side.

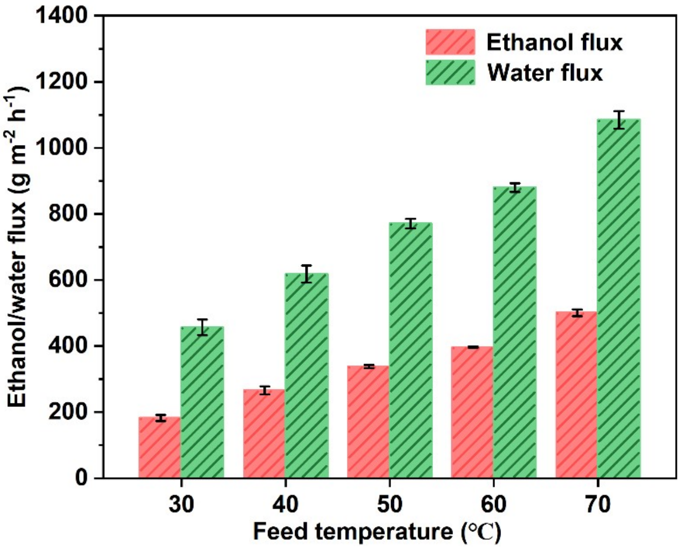

Fig. S19 Effect of feed temperation (30-70 °C) on PV performance using 5 wt% 1173IPS-MAPDMS membrane.

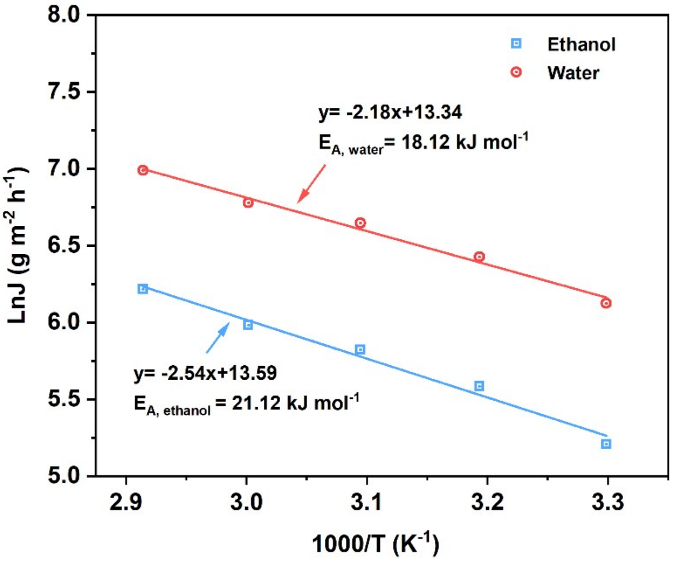

Fig. S20 Arrhenius plots of ethanol and water fluxes of the 5 wt% 1173IPS-MAPDMS membrane under 165 mW cm^{-2} for separating 5 wt% ethanol aqueous solution.

Table S6. Comparison of polymeric membranes in PV performance of ethanol/water separation.

Membrane	Feed temp. (°C)	Ethanol conc. (wt%)	Total flux (g m^{-2} h^{-1})	Separation factor	*PSI*	Ref.
PDMS	60	5	1186	8.2	8539	17
PDMS	70	5	1167	7.6	7702	18
PDMS	50	5	88	4.8	334	19
PDMS	50	5	800	5.8	3840	20
PDMS	60	5	886	6.8	5139	21
PDMS	60	5	225	7.5	1462	22
PDMS	30	5	850	6.2	4420	23
PDMS	55	5	500	4.5	1750	24
PDMS	40	5	500	7.5	3250	25
PDMS	37	6	450	6.9	2655	26
PDMS	40	5	1143	7.0	6858	27
PEBA[1]	40	5	1800	3.1	3780	28
PEBA[1]	40	5	833	3.6	2169	29
PEBA[1]	60	5	1650	4.0	4950	30
PEBA[1]	23	5	114	2.5	171	31
PEBA[1]	65	5	427	5.7	2007	32
PIM[2]	65	5	1240	6.4	6696	33
SBS[3]	40	10	15	5.4	66	34
SBS[3]	40	5	206	5.0	824	35
SBS[3]	40	10	33	5.6	151.8	36
PVB[4]	40	2.5	390	0.6	-	37
1173IPS-MAPDMS	60	5	1277	8.5	9575	This work
1173IPS-MAPDMS	60	5	1446	8.3	10614	This work
1173IPS-MAPDMS	70	5	1586	8.7	12260	This work

1: Poly (ether-*block*-amide)
2: Polymers of intrinsic microporosity
3: Polystyrene-*block*-polybutadiene-*block*-polystyrene
4: Poly(vinyl butyral)

Table S7. Energy required for PV process and evaporation process.

x_e (wt%)	y_e (wt%)	$\Delta H_{evap,e}$[1] (kJ kg^{-1})	$\Delta H_{evap,w}$[2] (kJ kg^{-1})	*Qnorm evap* (kJ kg^{-1})	Q'_{norm} (kJ kg^{-1})
5.0	31.06	918.2	2260	930.8	5934.4

1,2: The data of the evaporation enthalpy was from Xue *et al.*[38]

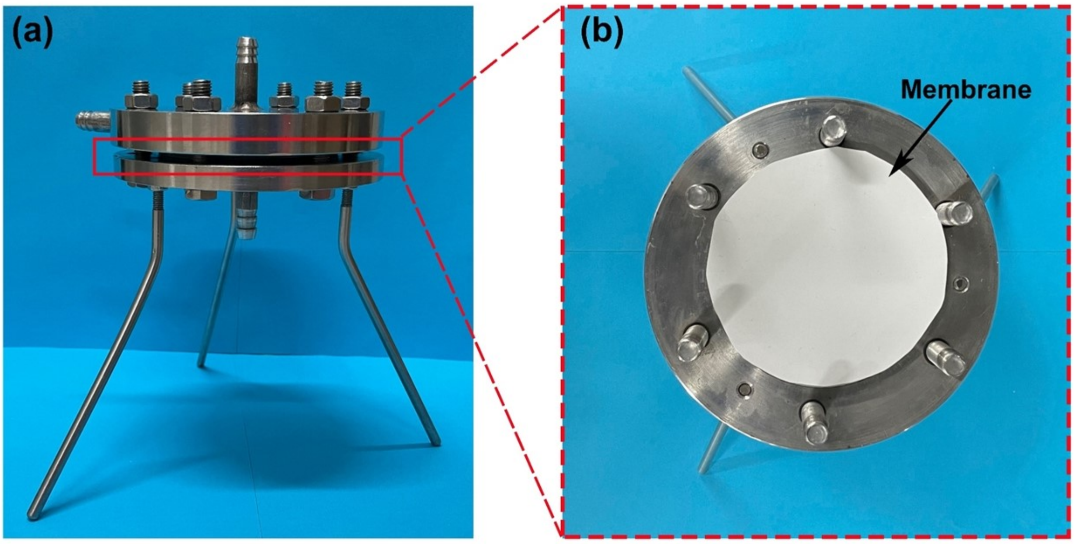

Fig. S21 **(a)** Digital photograph of the home-made membrane module, and **(b)** top view of the home-made membrane module.

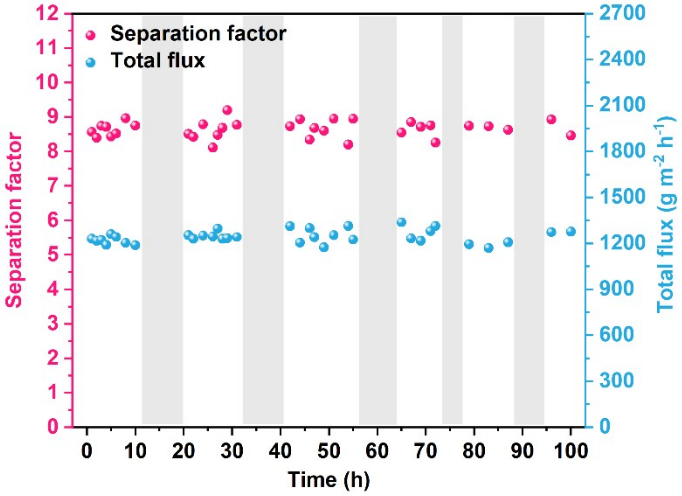

Fig. S22 Evaluations of durability and recycled times of membrane.

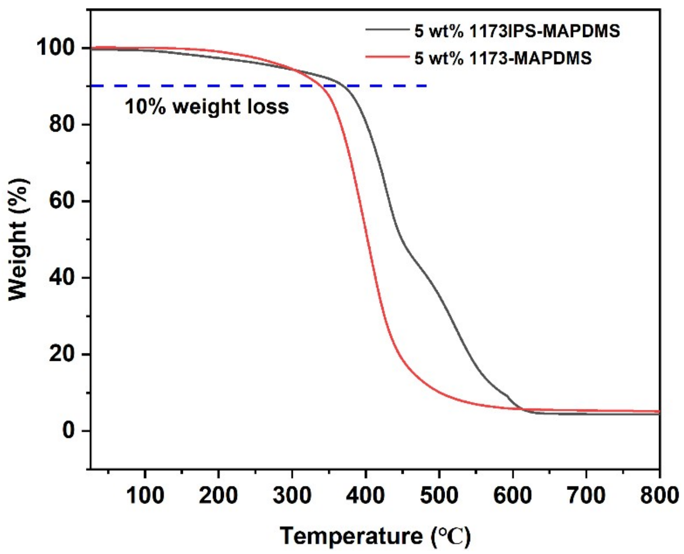

Fig. S23 TGA curves of 1173IPS-MAPDMS and MAPDMS membranes with 5 wt% PI.

1173IPS-MAPDMS membrane and MAPDMS membrane undergo two weight-loss stages. The first weight-loss stage is ascribed to the loss of $-CH_3$ from the Si-O backbone and the other side chains at 330-460 ℃. At 460-600 ℃, PDMS is decomposed to form siloxane and further a more stable carbon-like compound.[39]

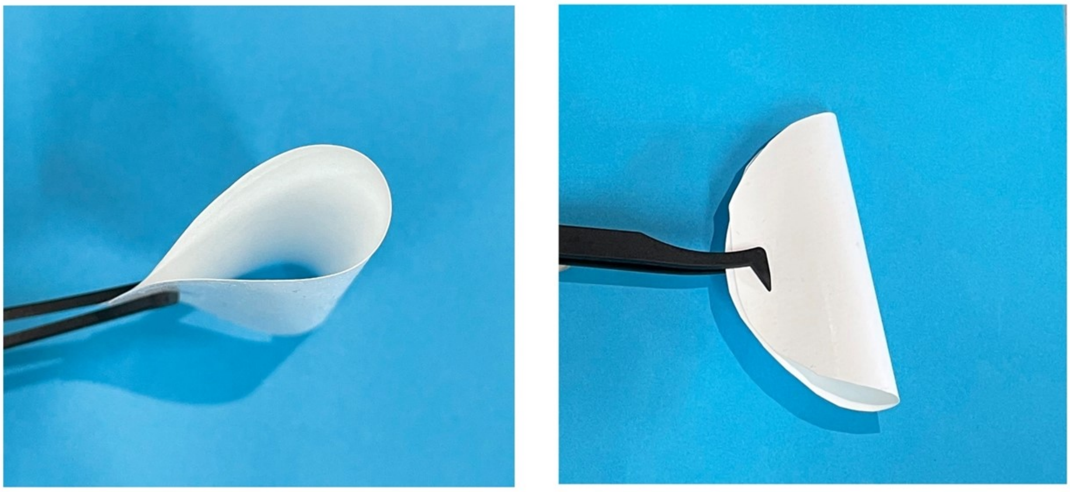

Fig. S24 Digital photographs of 5 wt% 1173IPS-MAPDMS membrane irradiated under 165 mW cm^{-2}.

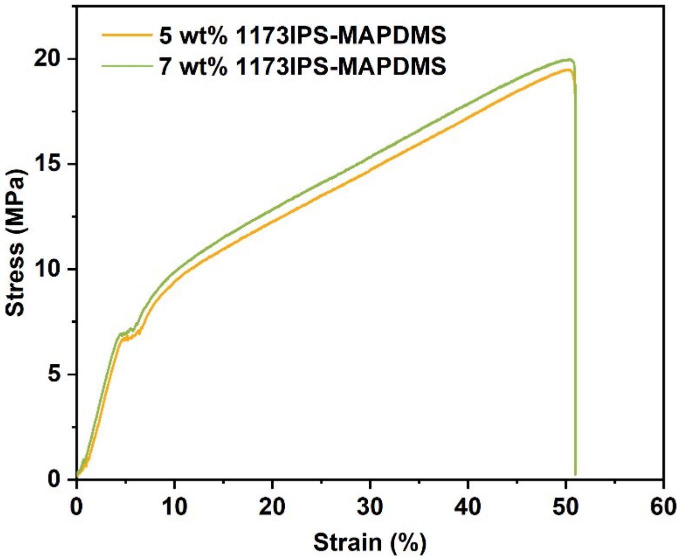

Fig. S25 The mechanical strength of 5-7 wt% 1173IPS-MAPDMS membrane irradiated under 165 mW cm^{-2}

The mechanical property of the used membrane is an important factor for practical application. In this work, the prepared membranes consist of three layers. The bottom layer, the middle layer, and the top layer are the nonwoven fabric layer, poly(vinylidene fluoride) (PVDF) porous layer, and 1173IPS-MAPDMS selectivity layer, respectively. PVDF is cast on the nonwoven fabric, and the formed composite structure is further used as the porous substrate.[40-43] Generally, the thin active layer (here refers to the 1173IPS-MAPDMS layer) of this composite membrane acts as the separating layer, and the porous substrate (here refers to the PVDF/nonwoven porous substrate) provides an enhancement in the mechanical strength.[26, 40, 44-46] As for the porous substrate, the nonwoven fabric provides a significant mechanical strength.[41] In fact, this composition membrane structure has been approved and widely used in commercial preparation,[43, 47-50] and its mechanical strength fully meets the requirements of practical application. For example, the commercial silicate-filled PDMS membrane (Pervap 1070) and the commercial PDMS membranes (Pervap 1070, Pervap 1060) fabricated by GFT (Sulzer Chemtech, Germany),[51-54] have been widely used in various PV applications, e.g., butanol recovery, phenol removal, toluene/water separation, and phenolic compounds recovery. In light of the analysis, the 1173IPS-MAPDMS membranes with the same composite structure in this work have a great mechanical strength to meet the practical requirement.

Table S8 Comparison of the mechanical strength for the reported polymeric membranes

Membrane	Mechanical properties			Ref.
	Tensile strength (MPa)	Elongation at break (%)	Elastic modulus (MPa)	
CTA[1]	12.3	5.6	-	55
PVA[2]	6.6	3.19	17	56
PVA[2]	11.3	8.80	-	57
NaAlg[3]	19.18	7.7	-	58
PDMS	4.7	22	-	59
PDMS	4.9	37	-	60
PDMS	0.89	38.54	3.97	25
PDMS	15.4	0.59	2.76	61
PDMS	0.88	38.56	3.67	62
PBS[4]	15.5	5.4	-	63
EPS[5]	6.8	3.5	-	64
5 wt% 1173IPS-MAPDMA	19.49	50.99	42.49	This work
7 wt% 1173IPS-MAPDMA	19.99	50.97	45.62	This work

1: Cellulose triacetate/cellulose nanocrystals
2: Poly(vinyl alcohol)
3: Sodium alginate
4: Polybutylene succinate
5: Exopolysaccharide

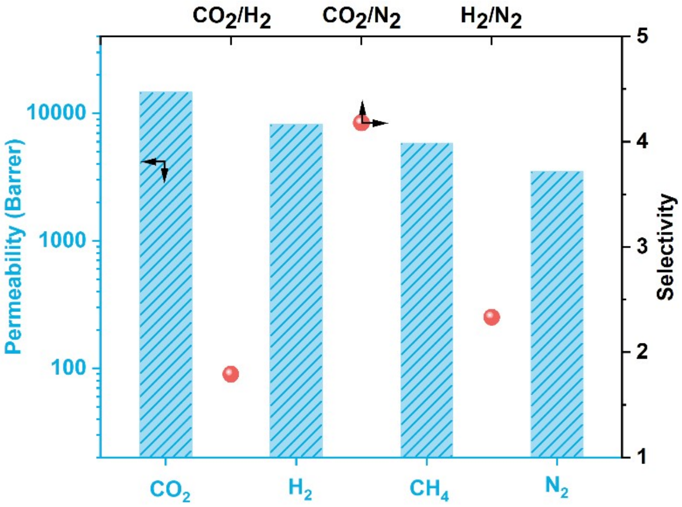

Fig. S26 Gas separation performance of 5 wt% 1173IPS-MAPDMS membrane (1 Barrer = 1× 10^{-10} cm^3 (STP) cm cm^{-2} s^{-1} $cmHg^{-1}$).

Table S9. Comparison of PDMS-type membranes in CO_2 and N_2 separation.

Membrane	Permeability (Barrer)		Ideal selectivity α	Test conditions	Ref.
	CO_2	N_2	CO_2/N_2		
PDMS	5500	-	1.42	35 °C, 0.5 bar	65
PDMS	20115	-	1.20	-	66
PDMS	759	-	2.66	25 °C, 20 bar	67
PDMS	4200	-	2.45	4 bar	68
PDMS	-	-	1.50	5 bar	69
PDMS	-	-	0.65	35 °C, 1 bar	70
PDMS	-	-	1.74	25 °C, 3.04 bar	71
PDMS	99400	30240	3.30	25 °C, 1 bar	72
PDMS	3170	-	1.50	35 °C, 2 bar	73
PDMS	169	-	1.63	22 °C, 2 bar	74
1173IPS-MAPDMS	14704	3517	4.18	35 °C, 1 bar	This work

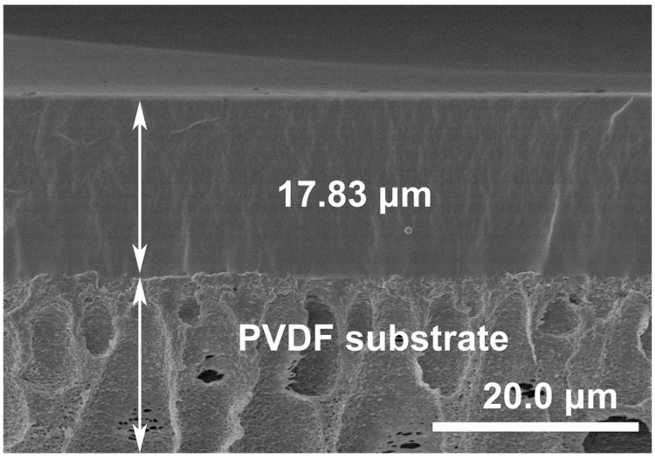

Fig. S27 SEM image of the cross-section of membrane made in a home-made coater.

The 1173IPS-MAPDMS membrane was fabricated in a home-made coater using PVDF substrate. The uniform and dense 1173IPS-MAPDMS layer is tightly adhered to the PVDF substrate, while the membrane thickness is 17.83 μm.

References

1. Z. Si, J. Li, L. Ma, D. Cai, S. Li, J. Baeyens, J. Degreve, J. Nie, T. Tan and P. Qin, *Angew. Chem. Int. Ed.*, 2019, **58**, 17175-17179.
2. W. Van Hecke, P. Vandezande, S. Claes, S. Vangeel, H. Beckers, L. Diels and H. De Wever, *Bioresour. Technol.,* 2012, **111**, 368-377.
3. R. Y. M. Huang, P. Shao, X. Feng and W. A. Anderson, *Ind. Eng. Chem. Res.*, 2002, **41**, 2957-2965.
4. L. Shao, T. Chung, S. Goh and K. Pramoda, *J. Membr. Sci.*, 2005, **265**, 46-56.
5. F. Zhou, Q. Dong, J. Chen, B. Sengupta, J. Jiang, W. L. Xu, H. Li, S. Li and M. Yu, *Chem. Eng. J.*, 2022, **430**, 132942.
6. J. J. Schwartz and A. J. Boydston, *Nat. Commun.*, 2019, **10**, 791.
7. W. Guo, Y. Jia, K. Tian, Z. Xu, J. Jiao, R. Li, Y. Wu, L. Cao and H. Wang, *ACS Appl. Mater. Interfaces*, 2016, **8**, 21046-21054.
8. L. Li, C. Lu, L. Wang, M. Chen, J. White, X. Hao, K. M. McLean, H. Chen and T. C. Hughes, *ACS Appl. Mater. Interfaces*, 2018, **10**, 13283-13292.
9. J. Wu, Y. Qian, C. A. Sutton, J. J. La Scala, D. C. Webster and M. P. Sibi, *ACS Sustainable Chem. Eng.*, 2021, **9**, 15537-15544.
10. W. Wang, Z. Liu, Z. Guo, J. Zhang, C. Li, S. Qiu, X. Lei and Q. Zhang, *ACS Appl. Mater. Interfaces*, 2020, **12**, 50812-50822.
11. E. Su, C. Bilici, G. Bayazit, S. Ide and O. Okay, *ACS Appl. Mater. Interfaces*, 2021, **13**, 21786-21799.

12. H. Gao, Y. Sun, M. Wang, Z. Wang, G. Han, L. Jin, P. Lin, Y. Xia and K. Zhang, *ACS Appl. Mater. Interfaces*, 2021, **13**, 1581-1591.

13. J. Xu, P. Lu, L. Wang, Y. Fan, W. Tian, J. Xu, J. Zhao, L. Ren and W. Ming, *J. Mater. Chem. A.*, 2021, **9**, 26028-26035.

14. L. Pezzana, G. Melilli, N. Guigo, N. Sbirrazzuoli and M. Sangermano, *ACS Sustainable Chem. Eng.*, 2021, **9**, 17403-17412.

15. P. Karami, C. S. Wyss, A. Khoushabi, A. Schmocker, M. Broome, C. Moser, P. E. Bourban and D. P. Pioletti, *ACS Appl. Mater. Interfaces*, 2018, **10**, 38692-38699.

16. H. Tan, D. Yang, J. Han, M. Xiao and J. Nie, *Appl. Clay Sci.*, 2008, **42**, 25-31.

17. H. Yan, J. Li, H. Fan, S. Ji, G. Zhang and Z. Zhang, *J. Membr. Sci.*, 2015, **481**, 94-105.

18. G. Zhang, J. Li, N. Wang, H. Fan, R. Zhang, G. Zhang and S. Ji, *J. Membr. Sci.*, 2015, **492**, 322-330.

19. Z. Zhu, D. Hu, Y. Liu, Y. Xu, G. Zeng, W. Wang, Y. Zhang and F. Cui, *J. Appl. Polym. Sci.*, 2017, **134**.

20. L. H. Wee, Y. Li, K. Zhang, P. Davit, S. Bordiga, J. Jiang, I. F. J. Vankelecom and J. A. Martens, *Adv. Funct. Mater.*, 2015, **25**, 516-525.

21. N. Wang, G. Shi, J. Gao, J. Li, L. Wang, H. Guo, G. Zhang and S. Ji, *Sep. Purif. Technol.*, 2015, **153**, 146-155.

22. X. Zhan, M. Wang, T. Gao, J. Lu, Y. He and J. Li, *Sep. Purif. Technol.*, 2020, **236**, 116238.

23. Y. Pan, T. Zhu, Q. Xia, X. Yu and Y. Wang, *J. Environ. Chem. Eng.*, 2021, **9**, 104977.

24. Y. Pan and X. Yu, *Sep. Purif. Technol.*, 2020, **237**, 116330.

25. H. Mao, H. Zhen, A. Ahmad, S. Li, Y. Liang, J. Ding, Y. Wu, L. Li and Z. Zhao, *J. Membr. Sci.*, 2019, **582**, 307-321.

26. X. He, T. Wang, Y. Li, J. Chen and J. Li, *J. Membr. Sci.*, 2018, **563**, 447-459.

27. A. J. Toth, B. Szilagyi, D. Fozer, E. Haaz, A. K. M. Selim, M. Szori, B. Viskolcz and P. Mizsey, *ACS Omega*, 2020, **5**, 15136-15145.

28. Q. Liu, Y. Li, Q. Li, G. Liu, G. Liu and W. Jin, *Sep. Purif. Technol.*, 2019, **214**, 2-10.

29. J. Gu, X. Shi, Y. Bai, H. Zhang, L. Zhang and H. Huang, *Chem. Eng. Technol.* 2009, **32**, 155-160.

30. A. Selim, K. Knozowska, B. Ośmiałowski, J. Kujawa, P. Mizsey and W. Kujawski, *Sep. Purif. Technol.*, 2021, **268**, 118707.

31. F. Liu, L. Liu and X. Feng, *Sep. Purif. Technol.*, 2005, **42**, 273-282.

32. N. Le, Y. Wang and T. Chung, *J. Membr. Sci.*, 2011, **379**, 174-183.

33. T. H. Butt, R. Tamime, P. M. Budd, W. J. Harrison, Z. Shamair and A. L. Khan, *Sep. Purif. Technol.*, 2022, **283**, 120216.

34. A. Kamtsikakis, S. McBride, J. O. Zoppe and C. Weder, *ACS Appl. Nano Mater.*, 2021, **4**, 568-579.

35. S. Santoro, F. Galiano, J. C. Jansen and A. Figoli, *Sep. Purif. Technol.*, 2017, **176**, 252-261.

36. A. Kamtsikakis, G. Delepierre and C. Weder, *J. Membr. Sci.*, 2021, **635**, 119473.

37. J. Li, M. Huang, P. Wei, Y. Zhang, X. Zhao, C. Liu, Z. Zhou and L. Zhang, *AIChE J.*, 2022, **68**, e17560.

38. C. Xue, J. Zhao, C. Lu, S. T. Yang, F. Bai and I. C. Tang, *Biotechnol. Bioeng.*, 2012, **109**, 2746-2756.

39. Q. Zhang, B. Fan, Q. Liu, A. Zhu and F. Shi, *J. Membr. Sci.*, 2011, **366**, 335-341.

40. R. W. Baker, *Membrane Technology and Applications*, John Wiley & Sons, Hoboken, 2012.

41. I. G. Wenten, K. Khoiruddin, G. T. M. Kadja, R. R. Mukti and P. D. Sutrisna, in *Polymer Nanocomposite Membranes for Pervaporation*, ed. T. Sabu, G. C. Soney and J. Thomasukutty, Elsevier, Netherlands, 2020, Ch. 11, 263-300.

42. C. Liu, T. Xue, Y. Yang, J. Ouyang, H. Chen, S. Yang, G. Li, D. Cai, Z. Si, S. Li and P. Qin, *Chem. Eng. Res. Des.*, 2021, **168**, 13-24.

43. Z. Si, H. Wu, P. Qin and B. Van der Bruggen, *Sep. Purif. Technol.,* 2022, **298**, 121612.

44. L. Gao, M. Alberto, P. Gorgojo, G. Szekely and P. M. Budd, *J. Membr. Sci.*, 2017, **529**, 207-214.

45. M. Mujiburohman, in *Polymer Nanocomposite Membranes for Pervaporation*, ed. T. Sabu, G. C. Soney and J. Thomasukutty, Elsevier, Netherlands, 2020, Ch. 14, 355-391.

46. T. Zhu, X. Yu, M. Yi and Y. Wang, *ACS Sustain. Chem. Eng.*, 2020, **8**, 12664-12676.

47. S. Li, F. Qin, P. Qin, M. N. Karim and T. Tan, *Green Chem.*, 2013, **15**, 2180.

48. G. Liu and W. Jin, *J. Membr. Sci.*, 2021, **636**, 119557.

49. G. Liu, W. Wei and W. Jin, *ACS Sustain. Chem. Eng.*, 2013, **2**, 546-560.

50. H. Zhu, G. Liu and W. Jin, *Energy Fuels*, 2020, **34**, 11962-11975.

51. E. A. Fouad and X. Feng, *J. Membr. Sci.*, 2009, **339**, 120-125.

52. W. Kujawski, A. Warszawski, W. Ratajczak, T. Porębski, W. Capała and I. Ostrowska, *Sep. Purif. Technol.*, 2004, **40**, 123-132.

53. S. V. Satyanarayana, A. Sharma and P. K. Bhattacharya, *Chem. Eng. J.*, 2004, **102**, 171-184.

54. P. Wu, R. W. Field, R. England and B. J. Brisdon, *J. Membr. Sci.*, 2001, **190**, 147-157.

55. I. Prihatiningtyas, Y. Li, Y. Hartanto, A. Vananroye, N. Coenen and B. Van der Bruggen, *Chem. Eng. J.*, 2020, **388**.

56. K. F. Yee, Y. T. Ong, A. R. Mohamed and S. H. Tan, *J. Membr. Sci.*, 2014, **453**, 546-555.

57. J. R. Karp, F. Hamerski and V. R. Silva, *Polym. Eng. Sci.*, 2018, **58**, 1879-1887.

58. S. D. Bhat and T. M. Aminabhavi, *J. Appl. Polym. Sci.*, 2009, **113**, 157-168.

59. H. Zhou, Y. Su, X. Chen, S. Yi and Y. Wan, *Sep. Purif. Technol.*, 2010, **75**, 286-294.

60. Q. Wu, Y. Sun, W. Wang, S. Tian, M. Ouyang, K. Chen, D. Shi, Y. Zhang, H. Li and Z. Zhao, *Sep. Purif. Technol.*, 2022, **298**, 121654.

61. H. Lee, Y. Lee, S. W. Lee, S.-M. Kang, Y. H. Kim, W. Jo, T.-S. Kim, J. Jang and B.-S. Bae, *Composites, Part B*, 2021, **225**, 109313.

62. H. Mao, S. Li, A. Zhang, L. Xu, J. Lu and Z. Zhao, *J. Membr. Sci.*, 2020, **595**, 117543.

63. H. Hashim Abed Almwli, S. M. Mousavi and S. Kiani, *Chem. Eng. Res. Des.*, 2021, **165**, 361-373.

64. I. T. Meireles, C. Brazinha, J. G. Crespo and I. M. Coelhoso, *J. Membr. Sci.*, 2013, **425-426**, 227-234.

65. J. Wang, Y. Li, Z. Zhang and Z. Hao, *J. Mater. Chem. A*, 2015, **3**, 8650-8658.

66. Y. Katayama, K. C. Bentz and S. M. Cohen, *ACS Appl. Mater. Interfaces*, 2019, **11**, 13029-13037.

67. B. Haider, M. R. Dilshad, M. Atiq Ur Rehman, J. V. Schmitz and M. Kaspereit, *Sep. Purif. Technol.*, 2020, **248**, 116899.

68. H. Wang, Y. Ni, Z. Dong and Q. Zhao, *React. Funct. Polym.*, 2021, **160**, 104825.

69. A. Jomekian, R. M. Behbahani, T. Mohammadi and A. Kargari, *Microporous Mesoporous Mater.*, 2016, **234**, 43-54.

70. M. He, J. Yao, Z. Low, D. Yu, Y. Feng and H. Wang, *RSC Adv.*, 2014, **4**, 7634.

71. S. S. Yoon, H. K. Lee and S. R. Hong, *Membranes*, 2021, **11**, 708.

72. P. Li, H. Z. Chen and T. Chung, *J. Membr. Sci.*, 2013, **434**, 18-25.

73. T. Hu, G. Dong, H. Li and V. Chen, *J. Membr. Sci.*, 2013, **432**, 13-24.

74. M. J. Yoo, K. H. Kim, J. H. Lee, T. W. Kim, C. W. Chung, Y. H. Cho and H. B. Park, *J. Membr. Sci.*, 2018, **566**, 336-345.